Changes in the Molecular Orientation and Tensile Properties of Uniaxially Drawn Cellulose Films

Wolfgang Gindl,*,† Klaus J. Martinschitz,‡ Peter Boesecke,§ and Jozef Keckes‡

Department of Materials Science and Process Engineering, University of Natural Resources and Applied Life Sciences, Vienna, Austria, Erich Schmid Institute of Materials Science, Austrian Academy of Sciences and Institute of Metal Physics, University of Leoben, Leoben, Austria, and European Synchrotron Radiation Facility, Grenoble, France

Received July 18, 2006; Revised Manuscript Received September 12, 2006

Cellulose films were prepared by dissolving lyocell fibers in LiCl/*N*,*N*-dimethylacetamide solvent and subsequently coagulating and drying them under ambient conditions. To introduce preferred orientation, the films were uniaxially drawn under air-dry and rewetted conditions, respectively. Preferred orientation was determined by birefringence measurements and by wide-angle X-ray scattering. Mechanical properties were characterized by means of tensile tests with films conditioned to standard temperatures and humidity. Drawing resulted in the substantial reorientation of cellulose, whereby the molecular chains in the amorphous regions exhibited clearly stronger reorientation than the crystalline fraction. The average degree of orientation was comparable to orientation achieved in spun cellulose fibers. Wet-drawing resulted in improved tensile strength and modulus of elasticity but reduced elongation at break. The mechanical properties of wet-drawn films are competitive with regard to cellophane and melt-blown cellulose films, particularly considering their high modulus of elasticity of up to 26 GPa, which is also comparable to values obtained for industrially produced cellulose fibers.

Introduction

Because of a rising demand for material features such as renewability, sustainability, and biodegradability, bio-based materials are increasing their importance, particularly with regard to composites.[1,2] In this context, cellulose, the most abundant biopolymer, is of particular interest.[3] The high stiffness and strength of cellulose make natural cellulosic fibers such as flax, hemp, ramie, and many others attractive reinforcement options for polymer composites.[4] This also applies to nanoscale cellulosic reinforcements such as microfibrillated cellulose, cellulose whiskers, and bacterial cellulose.[5] Nanoscale cellulosic reinforcements allow the production of composites with excellent strength of up to 400 MPa and an elastic modulus up to 28 GPa.[6] Besides the direct use of natural fibers and their nanoscale constituents for reinforcement, cellulose may also be dissolved and converted to films or spun into fibers.[7] Products made of regenerated cellulose show the advantage of less variability in shape and properties than natural cellulosic fibers, but are usually less stiff than the latter while being comparably strong. By controlling process parameters, the mechanical properties of regenerated cellulose fibers may be tuned within a wide range,[8,9] and a tensile strength of up to 1300 MPa and a tensile elastic modulus of up to 45 GPa (sonic modulus up to 58 GPa) may be achieved on the laboratory scale.[10] By comparison, regenerated cellulose films perform less well, particularly with regard to their modulus of elasticity. The properties of cellophane films are typically 5.4 GPa for the modulus of elasticity and 125 MPa for tensile strength, and up to 8 GPa and 300 MPa, respectively, for melt-blown cellulose films from *N*-methylmorpholine-*N*-oxide (NMMO) solution (lyocell process), depending on the degree of preferred orientation.[11] Recently it was shown that the stiffness of regenerated cellulose films can be significantly improved by incorporating undissolved cellulose I.[12] These films profit from the higher modulus of elasticity of cellulose I (138 GPa), which is typical of natural cellulose, compared to cellulose II (88 GPa), the crystalline conformation of regenerated cellulose.[13]

In the production of polymer films and fibers, preferred orientation, if desired, is introduced at some stage in order to achieve mechanical anisotropy.[14,15] A high degree of preferred orientation is desired for fibers, since they have to resist loads predominantly along their longitudinal axis. This general statement also holds true for the spinning of cellulosic fibers and for blown cellulosic films, where preferred orientation is introduced by stretching while cellulose desolvates. With an increasing draw ratio (D_R, the ratio between the length after stretching and the length before stretching), the degree of preferred orientation increases in regenerated cellulose fibers and films, and, in parallel, the elastic modulus and tensile strength increase, while the elongation at break decreases.[9,11] It was shown recently that a significant improvement in the modulus of elasticity of regenerated cellulose fibers may also be achieved by the plastic straining of fibers with an already consolidated structure.[16] Motivated by these results, uniaxial post-drawing was performed with regenerated cellulose films with consolidated structure and initially random orientation in the present study. We demonstrate that substantial reorientation of cellulose macromolecules achieved by this process causes significant improvement in the strength and modulus of elasticity.

Materials and Methods

Lyocell fibers with a linear density of 1.3 dtex were obtained from Lenzing R&D. For the production of cellulose films, the fibers were

* Corresponding author: Phone: ++43-1-47654-4255. Fax: ++43-1-47654-4295. E-mail: wolfgang.gindl@boku.ac.at.

† University of Natural Resources and Applied Life Sciences.

‡ University of Leoben.

§ European Synchrotron Radiation Facility.

10.1021/bm060698u CCC: $33.50
Published on Web 10/12/2006

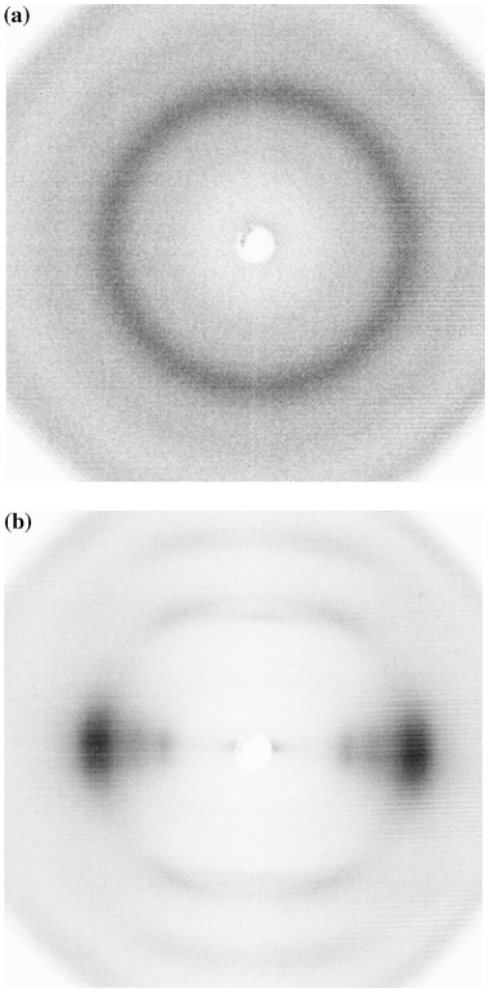

Figure 1. WAXS data from an unstretched cellulose film (a) and a film stretched to a draw ratio of 1.5 (b). The azimuthal distribution of intensity of the most intense cellulose II reflection (overlapping (110)/(020) reflection) is constant for the unstretched film (a), indicating random orientation. By contrast, strong maxima indicate preferred orientation of cellulose crystallites in the stretched film (b).

activated for 6 h in distilled H_2O at room temperature. Subsequently, the cellulose was dehydrated in ethanol, acetone, and *N*,*N*-dimethylacetamide (DMAc) for 4 h each. In parallel, a solution of 8 g of LiCl in 100 mL of DMAc was prepared. After decanting DMAc from the dehydrated cellulose, 100 mL of LiCl/DMAc solution was poured onto 2 g of cellulose fibers. The solution was stirred until dissolution of the lyocell fibers (10 min) and then poured into Petri disks (diameter = 20 cm) and left at an ambient atmosphere for 12 h. After this time, a 5 mm thick transparent gel had formed as a result of the uptake of water from ambient air, which leads to the desolvation of cellulose. The gelated films were washed in distilled water and dehydrated at an ambient temperature between gently compressed sheets of paper to a final dry film thickness of 0.11 mm.

For straining to introduce preferred orientation, the air-dry cellulose films were cut into strips of 50 mm length and 5 mm width. The strips were mounted to a Zwick 20 kN tensile testing machine and strained to a total strain of 9%, resulting in 6% permanent plastic strain upon unloading. This corresponds to a draw ratio (D_R, the ratio between specimen length after stretching and before stretching) of 1.06. To loosen the hydrogen bonding network and allow for more deformation, the cellulose films were immersed in distilled water for 5 min and subsequently stretched to draw ratios D_R of 1.1, 1.25, and 1.5 at a speed of 10 mm min^{-1} at an ambient temperature (20 °C). Draw ratios greater than 1.5 could not be obtained because of fracture of the strained films. In stretched conditions, the strips were dried by hot air in order to arrest the achieved elongation permanently and were subsequently

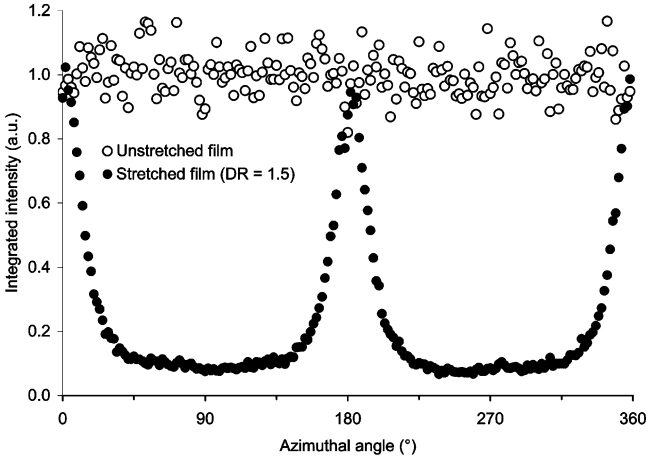

Figure 2. Example of the distribution of integrated intensity across the overlapping cellulose II (110)/(020) reflection as used for the calculation of the crystalline orientation parameter f_c.

released from the testing machine. Thereafter, all drawn specimens were left to equilibrate to ambient conditions (20 °C, 60% rel humidity) overnight. For mechanical testing, the specimens were again fixed to a tensile testing machine and tested at a speed of 1 mm min^{-1}. Strain was recorded by attaching Zwick-Macrosense clip-on strain sensors to the specimens. Drawn samples not tested in tensile testing were characterized by wide-angle X-ray scattering (WAXS) using a system Nanostar (Bruker AXS) with a beam diameter of 500 μm and a two-dimensional (2D) wire detector (Hi-Star). By radial integration of the intensity of the 2D detector images, 2θ profiles were obtained. The samples were rotated in the diffractometer, and additional 2θ profiles were obtained. From the profiles, crystallinity (x_c) was estimated from the ratio of crystalline scattering versus total scattering, whereby the amorphous contribution was estimated from an amorphous standard obtained by ball milling.

For comparison, single lyocell fibers were also tested in tension using a dedicated setup.[16] Single fibers were characterized in a synchrotron WAXS experiment performed at the beamline ID01 of the European synchrotron radiation facility (ESRF) in Grenoble, France. A radiation with a wavelength of 0.082 nm and a 2D detector with 1024 × 1024 pixels was used. The beam size on the sample was approximately 5 × 5 μm^2. The sample−detector distance was set to 96 mm.

Determination of Crystalline and Amorphous Orientation. To quantify the degree of preferred orientation of cellulose crystallites in the cellulose films and fibers, the azimuthal intensity distribution along the overlapping cellulose 110/020 reflection, which is at an angle of 90° with respect to the crystallographic *c*-axis of the cellulose crystal, was obtained by integrating the 2D detector WAXS images, as shown in Figure 1 using Fit2D software. The degree of preferred orientation derived from this reflection may be affected by the so-called leaflet effect.[11] This effect describes the phenomenon that, because of different dimensions of the cellulose crystallite, orientation may be different along the cellulose II (110)/(020) and the cellulose II ($1\bar{1}0$) reflection planes. However, we did not find statistically significant differences in the orientation factors derived from both reflections, which is why the most intense reflection (the cellulose II (110)/(020) reflection) was used. The degree of preferred orientation was determined by calculating the orientation factor $\langle \sin^2\phi \rangle$.[17] The integrated intensity distribution obtained numerically from WAXS patterns (Figure 2) was evaluated according to

$$\langle \sin^2\phi \rangle = \frac{\int_0^{\pi/2} I(\phi) \sin^3\phi \, d\phi}{\int_0^{\pi/2} I(\phi) \sin\phi \, d\phi} \quad (1)$$

where ϕ represents the azimuthal angle and $I(\phi)$ is the intensity along the 110/020 reflection. The factor $\langle \sin^2\phi \rangle$ equals 2/3 and 0 in the case

Table 1. Summary of Cellulose Film Properties Compared to a Lyocell Fiber

material	Δn	f_t	f_c	f_a	E (GPa)	σ_f (MPa)	ϵ_f (%)
undrawn film			0.00		8.5	201	19.6
film drawn wet ($D_R = 1.1$)	0.013	0.21	0.08	0.32	15.6	301	8.4
film drawn wet ($D_R = 1.25$)	0.024	0.38	0.14	0.59	21.3	358	6.8
film drawn wet ($D_R = 1.5$)	0.037	0.60	0.23	0.92	26.4	396	4.3
film drawn dry ($D_R = 1.06$)	0.008	0.14	0.05	0.21	9.9	199	8.3
lyocell fiber	0.039	0.63	0.96	0.43	24.5	585	8.2

[a] Draw ratio D_R, birefringence Δn, total orientation parameter f_t, crystalline orientation parameter f_c, amorphous orientation parameter f_a, modulus of elasticity E, tensile strength σ_f, and elongation at break ϵ_f.

of perfectly random and perfectly oriented structures, respectively.[17] Subsequently, the crystalline orientation parameter f_c was calculated from $\langle \sin^2\phi \rangle$ according to

$$f_c = 1 - \frac{3}{2}\sin^2\phi \tag{2}$$

Maximum orientation parallel to the fiber direction is found when $f_c = 1$, whereas $f_c = 0$ indicates random orientation.[17]

In addition to the crystalline orientation parameter f_c, the average orientation of both amorphous and crystalline cellulose was characterized by means of birefringence measurements using a Zeiss Axioimager microscope equipped with a Berek compensator 5λ. The specimen birefringence Δn was obtained by dividing the measured retardation of polarized light by the thickness of the specimen. The total orientation factor f_t was derived from Δn by dividing through the maximum birefringence of cellulose 0.062.[8] Subsequently, the degree of amorphous orientation f_a was obtained from eq 3:

$$f_a = \frac{f_t - (x_c \cdot f_c)}{(1 - x_c)\cdot 0.91} \tag{3}$$

where x_c stands for the crystallinity, which is 0.39 for the films produced here, and 0.91 corresponds to the ratio of the density of amorphous and crystalline domains.[18] It has to be mentioned at this point that the determination of amorphous orientation using eq 3 relies on certain assumptions regarding the maximum birefringence of crystalline and noncrystalline cellulose,[18] which in turn affect the accuracy of the absolute value of orientation factors determined here compared to methods such as polarized Raman spectroscopy,[19] whereas the relative change in orientation at different draw ratios should be correct.

Results and Discussion

Structural Changes in Drawn Cellulose Films. Structural characterization of the cellulose films produced in this study revealed significant changes in the arrangement of cellulose macromolecules due to plastic strain (Table 1). In films drawn in both wet and air-dry conditions, the orientation factor f_t derived from birefringence, which represents an average of the degree of orientation of crystalline and amorphous domains, increased with increasing draw ratio. However, the increase in preferred orientation was much more pronounced in films drawn in wet conditions than in dry conditions, which is explained by the higher chain mobility in water-swollen films due to weakening of intramolecular[20] and intermolecular hydrogen bonds due to the adsorption of water to accessible cellulose hydroxyl groups. Breaking down the total orientation factor f_t in its components f_c and f_a, which represent the degree of orientation of the crystalline and amorphous domains, respectively, reveals different reorientation intensities due to strain for these domains. Figure 3 consistently shows a higher degree of molecular orientation in amorphous domains compared to crystalline domains in all types of drawn films (i.e., wet and dry). Amorphous orientation reaches a high level of $f_a = 0.92$ in the film stretched by 50% ($D_R = 1.5$) in wet conditions, which is comparable to the magnitude of crystalline orientation f_c usually found in regenerated cellulose fibers.[11] Also Togawa and Kondo,[21] who performed stretching experiments with never-dried cellulose films of very low crystallinity, observed high amorphous orientation. Comparing the different pattern of orientation distribution found for crystalline and amorphous domains in plastically deformed cellulose films (Table 1, Figure 3) with the degree of preferred orientation typically found in regenerated cellulose fibers[11] and also in the lyocell fiber characterized for this study, a fundamental difference is apparent. A high degree of crystalline orientation ($f_c > 0.9$) is typical for regenerated cellulose fibers, together with significantly less orientation in amorphous domains,[11] which is in strong contrast to our results from films subjected to plastic tensile strain, where orientation is most pronounced in noncrystalline domains (Figure 3). This finding indicates a different mechanism of the development of orientation in fiber spinning compared to plastic straining of films with already consolidated structures, as performed in our study. In the spinning of cellulosic fibers, orientation is introduced by shear forces in the nozzle and by the difference in take-up speed and extrusion speed (draw ratio D_R). Because of relatively long relaxation times, orientation is largely preserved until consolidation of the structure by coagulation in the spinning bath.[11] In contrast, the structure of cellulose films studied here was already consolidated, since we started from isotropically oriented air-dry films.

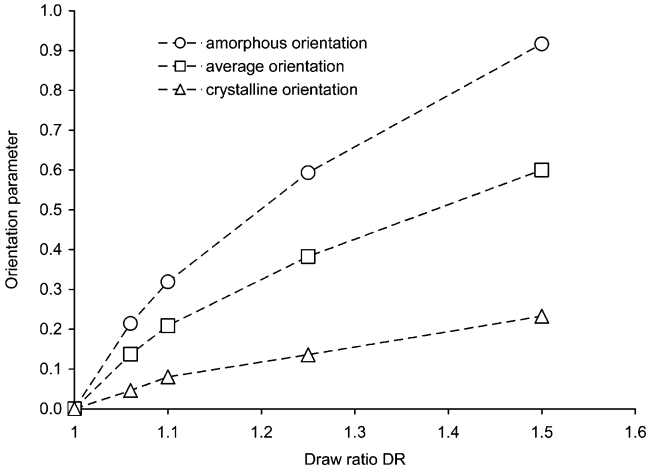

Figure 3. Effect of varying the draw ratio (D_R) on the crystalline orientation parameter f_c determined by WAXS, on the average orientation parameter f_t determined from specimen birefringence, and on the amorphous orientation parameter f_a calculated from f_c, f_t, and the specimen crystallinity (random orientation: $f_{c,t,a} = 0$; perfect orientation: $f_{c,t,a} = 1$).

The deformation behavior of semicrystalline polymers has been treated in a number of experimental and modeling studies.[19,22−27] An important component of most models is the concept of pseudo-affine deformation,[24] which assumes that molecular chains rotate under the global strain in a manner that the change in orientation of any chain segment parallel to a line drawn within the material would follow that of the drawn line. The model is termed pseudo-affine as opposed to affine because any change in length of the respective chain segment is ignored. This mechanism is described by eq 4:

$$\tan\phi = D_R^{3/2}\tan\phi' \tag{4}$$

where ϕ is the orientation angle of a unit before deformation

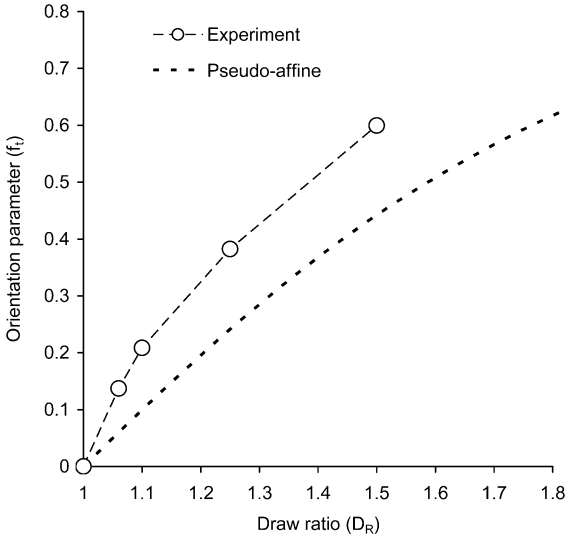

Figure 4. Comparison of the average degree of orientation f_t measured experimentally and the degree of orientation obtained assuming pseudo-affine deformation (eq 4).

and ϕ' is the corresponding orientation angle after a deformation with draw ratio D_R. Equation 4 was used to predict the degree of preferred orientation to be expected for cellulose films according to the draw ratios listed in Table 1. The resulting plot comparing model and experiment is shown in Figure 4. The model based on eq 4 underestimates the observed reorientation in our cellulose films. This indicates that additional parameters such as crystal slip and rotation should also be considered.[19,24] Nikolov et al.[27] point out that, in semicrystalline polymers, the deformation activity of the amorphous phase is initially higher than that of the crystalline phase at low strain, which may potentially serve as an explanation for the high degree of orientation found in the amorphous phase compared to the crystalline phase in our cellulose films (Figure 3). A similar pattern of higher amorphous than crystalline orientation upon drawing was found for polyvinyl alcohol[25] and polyethylene,[23,26] but the difference was much smaller than that found in the present study. The opposite pattern (i.e., higher crystalline orientation) was found for uniaxially drawn poly(lactic acid) films.[19] Apparently, the different orientation intensities of the crystalline and amorphous phases are strongly material-dependent. Upon deformation, cellulose behaves somewhat different from semicrystalline polymers studied above. In particular, cellulose does not show an increase in crystallinity with increasing draw,[21] as observed, for example, for poly(ethylene terephthalate).[28] No change in crystallinity was also observed for the cellulose films drawn in this study, with the crystallinity being persistently 0.39. In addition, in drawn semicrystalline polymers, the initial crystalline structure is eventually replaced by a stretched fibrillar structure,[27] a transition that was proposed to be absent in cellulose due to strong intermolecular hydrogen bonding.[21] In the present study, an evaluation of potential changes in lateral crystallite dimensions was not performed because 2θ scans of the WAXS 2D detector images from cellulose films stretched to different draw ratios (Figure 1) did not show significant changes in addition to experimental scatter, but were virtually identical. Thus, the specific structure and deformation behavior of cellulose may account for the difference observed between our experimental results and the pseudo-affine model.

Mechanical Properties. In parallel with the changes in structure of plastically deformed cellulose films discussed above, the mechanical properties were significantly affected by drawing.

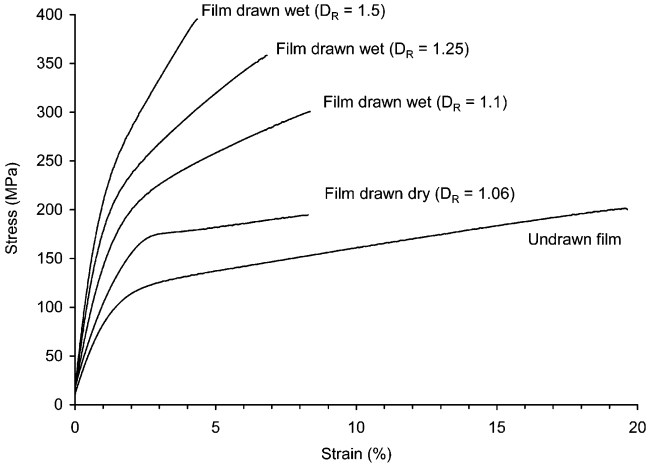

Figure 5. Stress−strain curves recorded in uniaxial tensile tests of cellulose films stretched to different draw ratios (D_R).

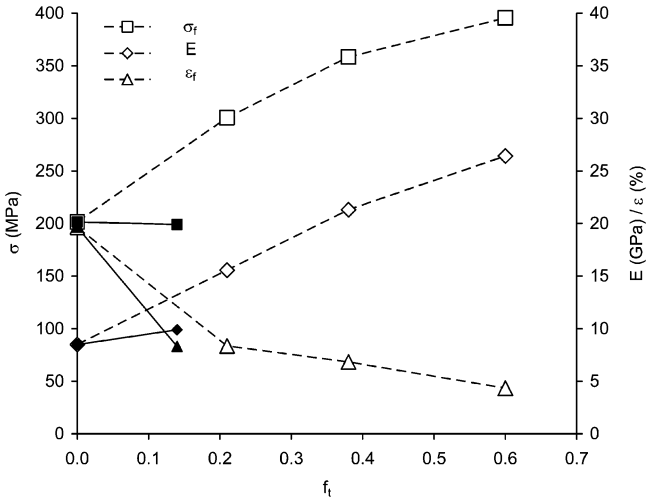

Figure 6. Relationship between the tensile strength (σ_f), the modulus of elasticity (E), the elongation at break (ϵ_f), and the average orientation parameter f_t (filled symbols and solid lines: films drawn dry; empty symbols and dashed lines: films drawn wet).

Figure 5 shows representative stress−strain curves for films stretched to different draw ratios. For films drawn in wet conditions, there is a clear tendency of increasing modulus of elasticity and tensile strength, and decreasing elongation at break with increasing draw ratio (Table 1, Figure 6), similar to what is observed for cellulose fibers stretched to varying degrees during spinning.[9] In contrast, drawing in dry conditions results only in a slight increase in the modulus of elasticity together with no significant change in tensile strength and clearly reduced failure strain (Table 1, Figure 6). This indicates that, in parallel to a certain degree of reorientation achieved during dry-drawing, which results in an improved modulus of elasticity, a certain amount of damage is possibly introduced into the film, which prevents a similar increase in the modulus, as observed in wet-drawn films, and hinders an improvement in tensile strength.

A comparison of the cellulosic films prepared for the present study with cellulosic fibers and other cellulosic films shows that wet uniaxial drawing is capable of producing films with excellent mechanical properties. When spun into fibers, a maximum tensile strength of 1.3 GPa and a modulus of elasticity of up to 45 GPa were observed for regenerated cellulose.[10] In practice, the mechanical properties of typical industrially produced cellulose fibers are in the range of 20 GPa for the modulus of elasticity and 830 MPa for tensile strength for rayon tire cords[29] and 22−24 GPa and 580−750 MPa, respectively,

for lyocell fibers (ref 16, Table 1). In contrast, the mechanical properties of cellulose films are usually less than those of fibers. Cellophane films typically show a value of 5.4 GPa for the modulus of elasticity and 125 MPa for tensile strength, whereas up to 8 GPa and 300 MPa, respectively, were observed for melt-blown cellulose films from NMMO solution (lyocell process), depending on the degree of preferred orientation.[11] With 26 GPa and 390 MPa, respectively, the cellulose films prepared by drawing in wet conditions in the present study perform very well with regard to cellophane and melt-blown films, particularly with regard to their modulus of elasticity, which is even comparable to values obtained for industrially produced cellulose fibers. The latter observation is very well explained by the comparable degree of average orientation measured for cellulose fibers and wet-drawn films.

Conclusion

From structural characterization and tensile testing of regenerated cellulose films uniaxially stretched at varying draw ratios in wet and air-dry conditions, we draw the following conclusions:

- Uniaxial drawing of cellulose films in wet conditions leads to a significant reorientation of cellulose chains in line with applied strain, the average degree of orientation obtained at $D_R = 1.5$ being comparable to that of spun cellulose fibers.
- While, in spun fibers, crystalline orientation is high compared to orientation in amorphous domains, the inverse is true for wet-drawn films, where orientation of the amorphous domains dominates.
- Wet-drawn cellulose films conditioned to ambient temperatures and moisture content show an increase in their modulus of elasticity and tensile strength, in parallel with a decrease in elongation at break related to an increasing draw ratio.
- The mechanical properties of wet-drawn films are competitive with other cellulosic films, clearly surpassing their modulus of elasticity.

References and Notes

(1) Gross, R. A.; Kalra, B. *Science* **2002**, *297*, 803−807.
(2) Mohanty, A. K.; Misra, M.; Drzal, L. T. *J. Polym. Environ.* **2002**, *10*, 19−26.
(3) Klemm, D.; Heublein, B.; Fink, H.-P.; Bohn, A. *Angew. Chem., Int. Ed.* **2005**, *44*, 2−37.
(4) Bledzki, A. K.; Gassan, J. *Prog. Polym. Sci.* **1999**, *24*, 221−274.
(5) Berglund, L. Cellulose-based nanocomposites. In *Natural Fibers, Biopolymers, and Biocomposites*; Mohanty, A. K., Misra, M., Drzal, L. T., Eds.; Taylor and Francis: Boca Raton, FL, 2005; pp 807−832.
(6) Nakagaito, A. N.; Iwamoto, S.; Yano, H. *Appl. Phys. A: Mater. Sci. Process.* **2005**, *80*, 93−97.
(7) Woodings, C. *Regenerated Cellulose Fibres*; Woodhead Publishing, Ltd.: Cambridge, U.K., 2001.
(8) Lenz, J.; Schurz, J.; Wrentschur, E. *Holzforschung* **1994**, *48* (Suppl), 72−76.
(9) Kong, K.; Eichhorn, S. J. *Polymer* **2005**, *46*, 6380−6390.
(10) Northolt, M. G.; Boerstoel, H.; Maatman, H.; Huisman, R.; Veurink, J.; Elzerman, H. *Polymer* **2001**, *42*, 8249−8264.
(11) Fink, H.-P.; Weigel, P.; Purz, H. J.; Ganster, J. *Prog. Polym. Sci.* **2001**, *26*, 1473−1524.
(12) Gindl, W.; Keckes, J. *Polymer* **2005**, *46*, 10221−10225.
(13) Nishino, T.; Takano, K.; Nakamae, K. *J. Polym. Sci., Polym. Phys.* **1995**, *33*, 1647−1651.
(14) Ward, I. M. *Structure and Properties of Oriented Polymers*; Applied Science Publishers: London, U.K., 1975.
(15) Ward, I. M. *J. Comput.-Aided Mater. Des.* **1997**, *4*, 43−52.
(16) Gindl, W.; Keckes, J. *Comput. Sci. Technol.* **2006**, doi: 10.1016/j.compscitech.2005.12.019.
(17) Alexander, L. E. *X-ray Diffraction Methods in Polymer Science*; Wiley-Interscience: London, U.K., 1969.
(18) Fink, H.-P.; Walenta, E. *Das Papier* **1994**, *12*, 739−748.
(19) Tanaka, M.; Young, R. J. *Macromolecules* **2006**, *39*, 3312−3321.
(20) Olsson, A.-M.; Salmen, L. *Carbohydr. Res.* **2004**, *339*, 813−818.
(21) Togawa, E.; Kondo, T. *J. Polym. Sci., Polym. Phys.* **1999**, *37*, 451−459.
(22) Crawford, S. M.; Kolsky, H. *Proc. Phys. Soc., London, Ser. B64* **1951**, *374*, 119−125.
(23) Bartczak, Z.; Galeski, A.; Argon, A. S.; Cohen, R. E. *Polymer* **1996**, *37*, 2113−2123.
(24) Ritchie, S. J. K. *J. Mater. Sci.* **2000**, *35*, 5829−5837.
(25) Matsuo, M.; Bin, Y.; Nakano, M. *Polymer* **2001**, *42*, 4687−4707.
(26) Hong, K.; Strobl, G. *Macromolecules* **2006**, *39*, 268−273.
(27) Nikolov, S.; Lebensohn, R. A.; Raabe, D. *J. Mech. Phys. Solids* **2006**, *54*, 1350−1375.
(28) Ajji, A.; Cole, K. C.; Dumoulin, M. M.; Ward, I. M. *Polym. Eng. Sci.* **1997**, *37*, 1801−1808.
(29) Ganster, J.; Fink, H.-P. *Cellulose* **2006**, *13*, 271−280.

BM060698U